EASR

Engineering and Applied Science Research

https://www.tci-thaijo.org/index.php/easr/index

Published by the Faculty of Engineering, Khon Kaen University, Thailand

Green-Synthesis and characterization of TiO_2 anatase nanoparticles as photocatalyst materials of methylene blue degradation

Munasir*[1)], Soffin Harjasa Setiawan Okto[1)], Nuhaa Faaizatunnisa[2)] and Fitriana[1)]

[1)]Department of Physics, Faculty of Mathematics and Natural Sciences, Universitas Negeri Surabaya, Kampus Ketintang, Surabaya 60231, East-Java, Indonesia
[2)]Department of Chemistry, Faculty of Science and Data Analytics, Institut Teknologi Sepuluh Nopember, Kampus ITS Keputih-Sukolilo, Surabaya 60111, East-Java, Indonesia

Received 2 December 2024
Revised 1 May 2025
Accepted 7 May 2025

Abstract

Water pollution is a critical global issue, hindering the achievement of SDG-6 on clean water and sanitation. Titanium dioxide (TiO_2) nanoparticles (NPs) have emerged as effective photocatalysts for degrading organic pollutants. Green synthesis, utilizing plant-derived phytochemicals as natural reducing and capping agents, offers an eco-friendly alternative to conventional methods. This study reports the green synthesis of TiO_2 NPs using just (*Syzygium cumini*) leaf extract as a reductant. The synthesized nanoparticles were characterized using XRD, XRF, FTIR, UV-Vis, bandgap analysis, SEM, and TEM. The results confirmed the formation of anatase-phase TiO_2 with 98.21% purity (XRF), a spherical morphology (≈10-50 nm), and a bandgap of 2.94 eV. Photocatalytic tests demonstrated 94.92% and 95.89% methylene blue degradation efficiencies after 180 and 240 minutes under UV light. These findings highlight the potential of green-synthesized TiO_2 NPs for environmental remediation. Future studies should explore modifications to enhance photocatalytic performance for wastewater treatment applications.

Keywords: Green synthesis, TiO_2-Anatase, Photocatalyst, Water treatment, SDGs-6

1. Introduction

The availability of clean water has become a global challenge, with some regions experiencing severe water shortages while others suffer from contamination due to household and industrial waste. This issue poses a significant barrier to achieving the 6th Sustainable Development Goal (SDG), which aims to ensure access to clean water and sustainable sanitation for all [1-3]. Among the major contributors to water pollution are effluents from textiles [4], pharmaceutical [5, 6], and household industries [7], which release various pollutants such as starch, drying agents, waste treatment by-products, boiling agents, dyes, and finishing materials [8]. Textile dyes, particularly synthetic dyes, are widely used due to their availability, diverse color variations, and ease of application [9]. However, these dyes pose environmental risks as they degrade into toxic compounds that threaten ecosystems [10]. Methylene blue (MB) is a commonly used cationic dye with applications in chemistry, biology, medicine, and the textile industry [11]. Despite its advantages, MB exhibits high chemical stability due to its benzene structure, making it difficult to degrade naturally [12-14]. MB in wastewater can lead to severe environmental and health issues [15], including digestive tract irritation, cyanosis, and skin irritation upon exposure. Therefore, efficient methods for MB degradation are urgently needed, with photocatalysis emerging as a promising approach [16].
Photocatalysis has gained significant attention for degrading organic pollutants, including MB. This method utilizes semiconductor materials as photocatalysts to accelerate the breakdown of complex pollutants under light irradiation [17]. Among various photocatalysts, titanium dioxide (TiO_2) is widely recognized for its excellent optical properties, non-toxicity, affordability, and high thermal and mechanical stability [18]. The nanoscale size of photocatalyst materials further enhances pollutant degradation efficiency by increasing surface area and reactivity [19].

Recently, the development of green-synthesized nanoparticles has emerged as an eco-friendly alternative to conventional synthesis methods. Green synthesis eliminates or significantly reduces the use of toxic chemicals, thereby minimizing environmental pollution and health risks [19-21]. Additionally, plant-based reducing agents provide a renewable and biodegradable alternative, enhancing cost efficiency and sustainability [22]. The bioactive compounds in plant extracts contribute to improved nanoparticle stability, dispersibility, and catalytic efficiency, making them highly effective for drug delivery, antimicrobial treatments, and photocatalysis [1, 16, 23-26]. Various plant-based bio-reductants, particularly those used in the synthesis of TiO_2 nanoparticles, such as *Portulaca oleracea*, *Zea mays*, *Bixa Orellana*, *Moringa oleifera*, *Neem* leaves, and *Luffa acutangular* [22-31], have demonstrated remarkable versatility in green synthesis approaches, enabling the production of nanoparticles with tunable properties suitable for diverse applications.

*Corresponding author.
Email address: munasir_physics@unesa.ac.id
doi: 10.14456/easr.2025.36

Among different synthesis routes, green synthesis of TiO_2 nanoparticles using plant extracts presents a sustainable and straightforward approach. This method leverages bioactive compounds as natural reducing agents to facilitate nanoparticle formation [21, 29, 32]. TiO_2 has three polymorphic forms: anatase, rutile, and brookite, each with distinct bandgap energies [9, 33-35]. Anatase, with a bandgap energy of 3.2 eV, is particularly suitable for photocatalytic applications due to its high electron mobility and reduced electron-hole recombination rate, making it a preferred choice for environmental remediation. Juwet (*Syzygium cumini*) leaf extract has emerged as a potential bio-reductant for green synthesis due to its rich composition of bioactive compounds, including alkaloids, flavonoids, tannins, and essential oils [36]. These compounds, particularly flavonoids and phenols, possess hydroxyl (-OH) groups that facilitate electron transfer, playing a crucial role in the reduction of Ti^{4+} ions to Ti^{3+} [37, 38]. However, research on using juwet leaf extract for TiO_2 synthesis remains limited. Conventional TiO_2 synthesis methods often involve hazardous reagents and energy-intensive processes, highlighting the need for greener alternatives.

This study explores the green synthesis of TiO_2 nanoparticles using just leaf extract as a natural bio-reductant and evaluates their photocatalytic performance in methylene blue degradation under UV light. By investigating the impact of plant-derived bioactive compounds on TiO_2 properties, this study aims to introduce a more environmentally friendly synthesis method and contribute to the advancement of sustainable nanotechnology for environmental applications.

2. Materials and methods

2.1 Materials

Titanium isopropoxide (TTIP, Sigma-Aldrich, 97%); Juwet leaves (*Syzygium cumini* L.) containing flavonoids (0.417% by weight), saponins (0.766% by weight), tannins (0.282% by weight), alkaloids (0.384% by weight) [39]; distilled water and methylene blue (Sigma-Aldrich, dye content ≥82%).

2.2 Preparation juwet leaf extract

The synthesis process of TiO_2 nanoparticles began with the preparation of juwet leaf extract. The juwet leaves were oven-dried at 60°C for approximately 60–90 minutes until completely dry and turned brown. The dried leaves were then blended into a fine powder, which was used for the extraction process. For extraction, 20 g of juwet leaf powder was added to 150 ml of distilled water and stirred using a magnetic stirrer at 80°C for 60 minutes. The solution was then cooled to room temperature and filtered using a vacuum filtration setup to obtain the filtrate of juwet leaf extract (Figure 1). 75 ml of extract was obtained as the reducing agent for TiO_2 nanoparticle synthesis. The juwet leaf extract, known for its medicinal properties, contains secondary metabolites such as alkaloids, phenols, flavonoids, steroids, tannins, resins, and carbohydrates [40].

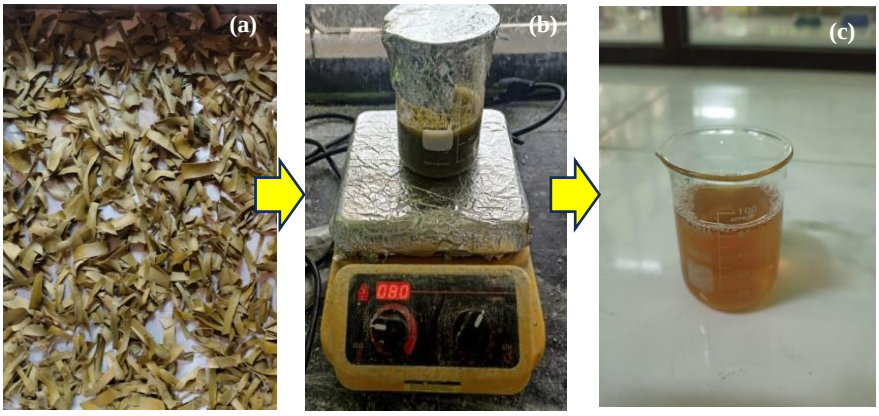

Figure 1 Extraction of Juwet Leaves: (a) Juwet leaves after drying (b) Process of mixing juwet leaves with distilled water (c) Extraction that has been filtered.

2.3 Green synthesis of TiO_2 nanoparticles

A total extraction of 75 ml was obtained, which will then be used as a TiO_2 nanoparticle reducer. After getting a reducer from juwet leaf extract, juwet leaf extract is mixed with Titanium isopropoxide (TTIP) as a precursor for TiO_2 synthesis. Mix precursors and reducers using a volume ratio of 1:1, namely 75 ml of juwet leaf extract with 75 ml of TTIP. Furthermore, the mixture was stirred using a stirrer at room temperature for 8 hours until the solution reached a homogeneous state. After the stirring process, the mixture was centrifuged at 3000 rpm for 10 minutes to separate the wet powder and filtrate. The collected precipitate was dried at 100°C for 8 hours and then calcined at 570°C for 3 hours. This temperature was chosen to ensure the formation of high-purity, well-crystallized anatase TiO_2 with excellent photocatalytic efficiency while preventing unwanted phase transformation to rutile [41]. The mechanism synthesis of TiO_2 nanoparticles can be seen in Figure 2.

2.4 Characterization of TiO_2 NPs

The synthesized TiO_2 nanoparticles were then characterized by X-ray diffraction (XRD), type X-Ray Diffraction (XRD) PANalytical Brand, Type: X'Pert PRO, for analysis of the crystal phase of TiO_2 produced and crystal size. X-Ray Fluorescence (XRF), type: PANalytical, Type: Minipal 4; to analyze the purity of TiO_2 oxide obtained by Green synthesis with juwet leaf extract. Fourier Transform InfraRed (FTIR) analyzed Ti-O functional groups using Shimadzu-type IR Prestige-21 instrumentation (Kyoto, Japan). UV-

Vis spectroscopy was used to analyze the wavelength area, and bandgap with the Tauc-plot equation can be written as $(\alpha hv)^{1/2} = D(hv - Eg)$ [42] and used in the photocatalysis process to determine the absorbance value of methylene blue solution before and after photocatalysis treatment. Scanning Electron Microscope-Energy Dispersive X-ray (SEM-EDX), type: Scanning Electron Microscopy (SEM) FEI Brand, Type: Inspect-S50; used to analyze the morphology and dominant elements of the obtained TiO_2 powder; and Transmission Electron Microscopy (TEM), type: Jeol Jem-1400; for analysis of morphology, shape, and size of TiO_2 particles.

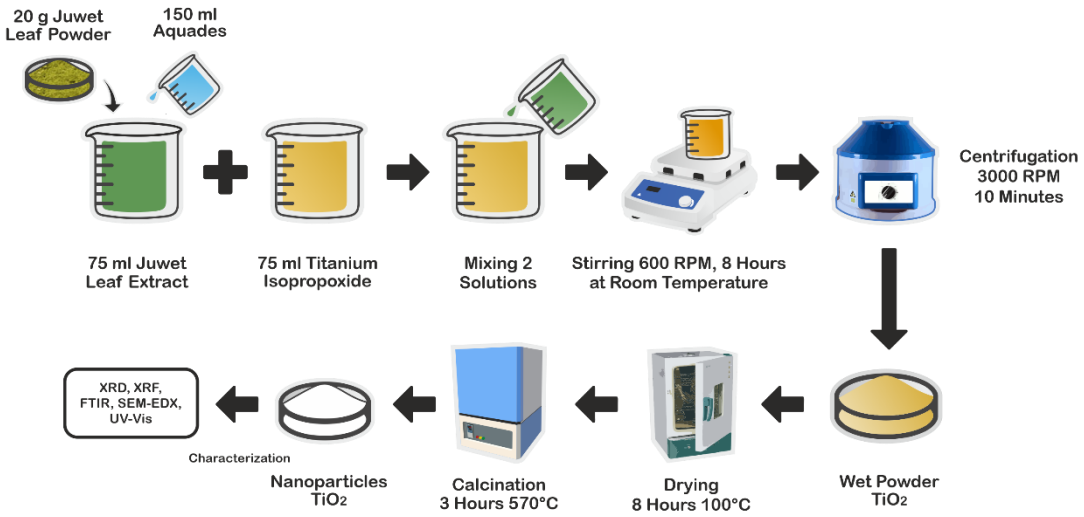

Figure 2 Mechanism Synthesis of TiO_2 Nanoparticles Using the Green Synthesis Method

2.5 Photocatalysis Performance of TiO_2 NPs

The adsorption study of the synthesized TiO_2 NPs on MB in water was conducted in a batch system with an initial MB concentration of 30 ppm at 10 mg/L and an adsorbent dosage of 0.01 grams in 50 mL for 240 minutes. Additionally, the adsorption process was carried out at various contact times (0, 10, 20, 30 minutes) to determine the equilibrium adsorption time, which was then used as the duration of dark conditions in the photocatalytic process. The irradiation time was varied at 60, 120, 180, and 240 minutes. The remaining MB concentration in the solution was measured using a UV-Vis spectrophotometer at a wavelength of 664 nm. To determine the percentage of dye degradation by TiO_2 nanoparticles used the equation (Eq. 1) [42, 43]:

$$\%\, Efficiency\ photocatalyst = \frac{C_o - C_t}{C_o} \times 100\% \quad (1)$$

where C_o is the initial concentration of methylene blue, and C_t is the final concentration of methylene blue after the photocatalysis process (mg/L).

3. Results and discussion

3.1 Green-Synthesis nanoparticle TiO_2

As a semiconductor material, titanium dioxide (TiO2) has good chemical and thermal stability, low cost, and high photocatalytic efficiency with an energy band gap of ~3.2 eV [18]. TiO_2 can be synthesized using a green synthesis method, which is quite simple, economical, non-toxic, and environmentally friendly because the chemical reactants are replaced using natural materials, namely plant extracts such as leaves [19] and aloe vera [30]. Aloe vera extract contains aloe emodin, lignin, hemicellulose, and pectin compounds which function as reducing agents in the formation of TiO_2 nanoparticles [44]. The reduction of Ti^{4+} by plant extracts forms TiO_2 nanoparticles, which are stabilized by plant metabolites to prevent agglomeration and enhance stability (Figure 3). In this case, the metabolites present in Juwet leaf extract, such as flavonoids, act as bioreductors and capping agents for TiO_2 nanoparticles, contributing to the reduction of Ti^{4+} to TiO_2 and simultaneously stabilizing the nanoparticles to prevent aggregation. Additionally, green synthesis is economical and sustainable due to readily available natural materials, minimizing the need for expensive and toxic chemicals. These methods generally operate under ambient conditions, reducing energy consumption compared to conventional synthesis, making the process more energy-efficient and environmentally friendly.

Meanwhile, juwet leaves are reported to contain very important chemical compounds and play an effective role in the process of reducing Ti ions in precursors (TTIP) are phenol and flavonoids because they contain hydroxyl groups (-OH) that easily release electrons [45-47]. Phenol has a hydroxyl group bound to an aromatic ring, so it is very reactive in redox reactions and reduces metal ions such as Ti^{+4}. Likewise, flavonoids are polyphenolic compounds with antioxidant properties, and their hydroxyl groups release electrons to reduce metal ions (such as Ti^{+4}) [38].

3.2 Pattern XRD analysis

XRD characterization analysis was carried out to determine the structure of the diffraction pattern formed in TiO_2 NPs. The results are the diffraction peak (2θ), diffraction intensity, and Miller index.

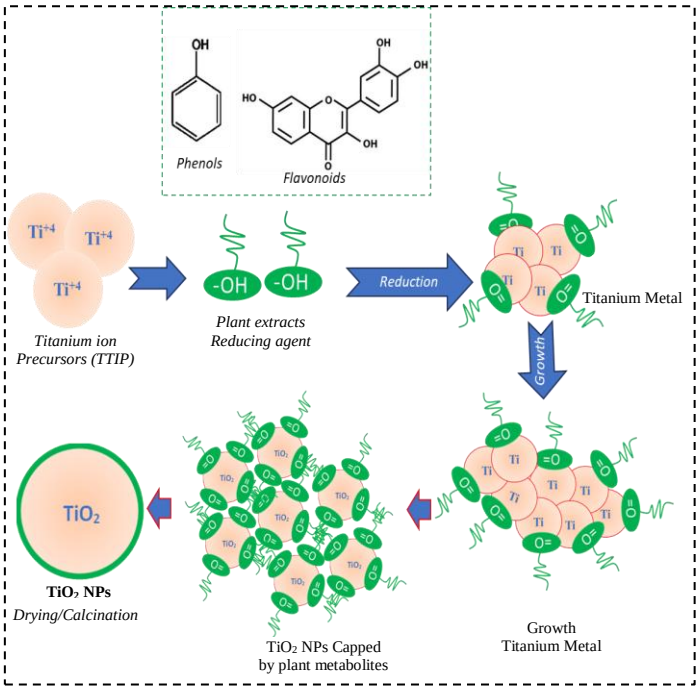

Figure 3 Synthesis mechanism of TiO_2 nanoparticles using green-synthesis method

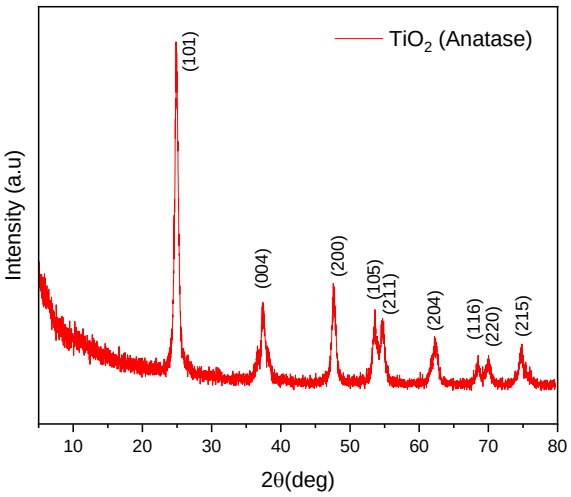

Figure 4 XRD characterization of TiO_2 (*anatase crystalline*)

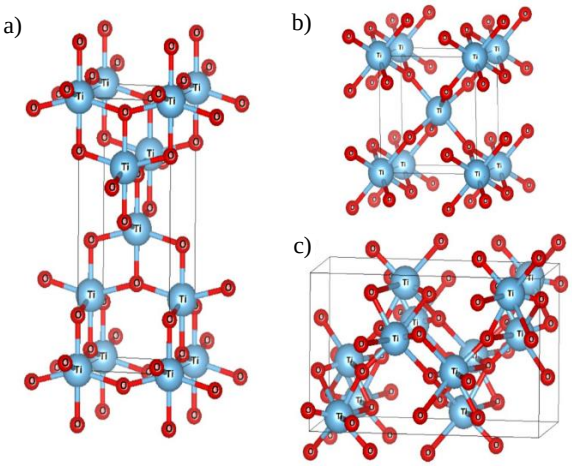

Figure 5 Crystal structures of TiO_2 (a) anatase (tetragonal), (b) rutile (tetragonal), and (c) brookite (orthorhombic) polymorphs (Computational Models: 3-D)

Based on Figure 4, XRD characterization of the TiO_2 diffraction pattern shown in the red image, there are diffraction peaks in the range of $5° < 2\theta < 80°$, namely 25.30°; 36.94°; 37.79°; 38.60°; 48.03°; 53.88°; 55.02°; 62.68°; 68.82°; 70.32°; 74.99° and each peak has a miller index value (hkl) as follows: (101), (103), (004), (112), (200), (105), (211), (204), (116), (220), (215). These results correspond to the characteristic peaks of the anatase TiO_2 phase based on the reference data from JCPDS (Card No. 72-06075) and are consistent with the findings reported in previous studies [36, 48, 49]. The average crystallite size of TiO_2 nanoparticles was found to be 15.7 nm. The size of TiO_2 crystals is nano-sized because materials with sizes less than 100 nm can be categorized as nanocrystallites [42]. Figure 5 shows the crystal structure model of TiO_2: anatase, rutile, and brookite (3-D). It can be seen that the tetragonal structure of anatase (space group $I4_1/amd$) is more elongated (c-axis) compared to the tetragonal rutile (space group $P4_2/mnm$), which is more compact. At the same time, brookite forms an orthorhombic crystal space (space group Pbca).

3.3 XRF analysis

XRF characterization analysis was used to identify the compound content in the TiO_2 nanoparticles synthesized with the help of reducing juwet leaf extract. This method includes the analysis of elements and oxides contained in the sample. The working principle of XRF characterization involves the interaction of X-rays with the analyte material, which allows the identification of the elements and oxides that make up the material. Elements can be identified directly without the need for specific standards. From pattern diffraction-XRF, information can be obtained about the content of most of the elements in TiO_2 nanoparticles, including the element Ti and some of its elements. However, only a few other elements are present in TiO_2 nanoparticles, so TiO_2 nanoparticles synthesized using juwet leaf extract have good elemental purity as a nanoparticle material.

Table 1 Results of Oxide Content Analysis on TiO_2 Using XRF

Senyawa (Oksida)	P_2O_5	K_2O	CaO	TiO_2	WO_3	OsO_4	PtO_2
(%)	0,21	0,20	0,26	**98,21**	0,27	0,67	0,17

Based on Table 1, the results of the oxide content analysis show that in TiO_2 nanoparticles, the compound with the largest content is titanium dioxide (TiO_2), which is 98.21%. Several other compounds are also contained in TiO_2 nanoparticles, such as P_2O_3, K_2O, CaO, OsO_4, and PtO_2. However, the percentage content of these compounds is less than 1%, so it is classified as very low. Therefore, the synthesis process of TiO_2 nanoparticles using Juwet leaf extract has the potential to be a good candidate for nanoparticle material with a purity level of 98.21%.

3.4 FTIR analysis

FTIR characterization is used to determine the presence of functional groups of TiO_2 nanoparticles. The spectrum of FTIR characterization results is the relationship between wave number and transmittance. Figure 6 shows the results of FTIR characterization of TiO_2, namely the absorption band that appears at the length of 414.71 cm^{-1} and 475.47 cm^{-1}, which shows the stretching vibrations of the Ti-O and Ti-O-Ti bonds which indicate the presence of TiO_2. The large peak at 3413.19 cm^{-1} and the small peak at 1628.95 cm^{-1} indicate the presence of O-H and C-OH hydroxyl functional groups (only dominant in TiO_2 NPs prepared by the green synthesis method). This hydroxyl group can absorb the water surface so that this group can support the process of TiO_2 photocatalyst activity [36, 50].

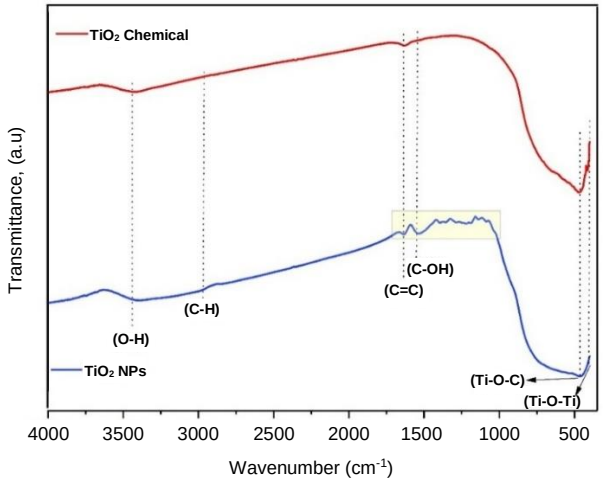

Figure 6 FTIR of TiO_2 NPs: green synthesis and chemical preparations

Table 2 Comparison Table of FTIR Test Results with Literature

Wavenumber (cm^{-1})	Functional Groups	Wavenumber (cm^{-1})	Ref
414,71	Ti-O (stretching)	414	[51]
475,47	Ti-O-Ti (stretching)	482	[50]
1628,95	C-OH (hydroxyl)	1628	[36]
3413,19	O-H (hydroxyl)	3400	[52]

3.5 SEM-EDX analysis

Scanning Electron Microscope -Energy Dispersive X-ray (SEM-EDX) characterization is used to determine the morphology of a material as well as the particle size of the material. Based on the SEM image in Figure (7a), TiO_2 nanoparticles synthesized using Juwet leaf plant extract bioreductor show aggregation morphology with a non-uniform shape. The particles appear almost spherical with varying nano sizes [37]. This aggregation is likely caused by Van der Waals forces between nanoparticles or the presence of residual organic compounds from plant extracts that function as stabilizing agents during synthesis. Compared to conventional methods such as sol-gel or precipitation without biological agents, plant extract-based synthesis produces nanoparticles with a broader size distribution and higher aggregation. However, this method has advantages in sustainability and is environmentally friendly because it does not require hazardous chemicals [53].

The average diameter value calculated using ImageJ software, as shown in the histogram diagram in Figure 7(b), shows the particle size distribution of TiO_2 with a range of about 6-15 nm, with the peak of the distribution at around 10.50 nm. The fit curve shows a right-skewed distribution, indicating the presence of larger particles affecting the overall distribution. Compared with other studies, several studies have reported that synthesizing TiO_2 NPs using plant extracts can produce particle sizes ranging from 10–100 nm depending on the type of extract and the synthesis parameters used. For example, the synthesis of TiO_2 using Moringa leaf extract produces particles with a size of 20–80 nm with a more uniform shape [54]. In contrast, green tea leaf extract produces larger particle sizes with a higher degree of aggregation. The EDX mapping (Figure 7(c)) results show the presence of titanium (Ti) and oxygen (O) with an atomic percentage of 22.8% and 77.2%, respectively, which is further confirmed by the XRF analysis results (Table 1).

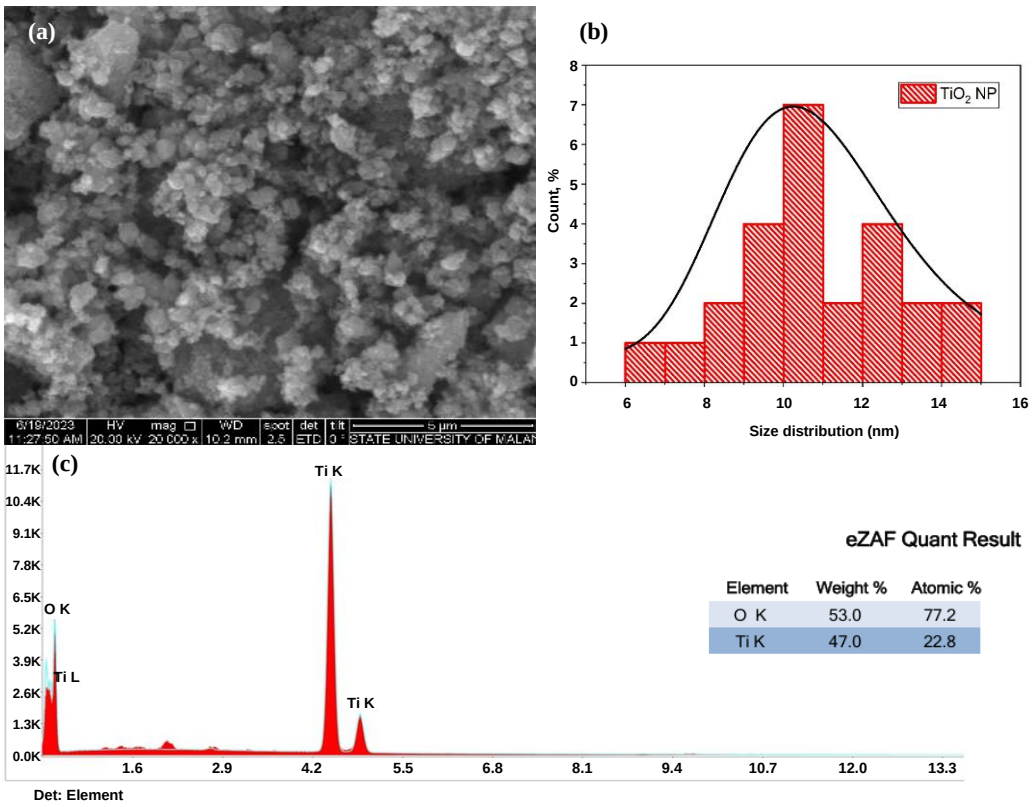

Figure 7 SEM characterization results of TiO_2: (a) Morphology of TiO_2 with 20kx magnification (b) Histogram of TiO_2 particle size; and (c) EDX mapping, with an atomic percentage: Ti (22.8 %) and O (77.2%)

TEM analysis in Figure 8 shows TiO_2 nanoparticles synthesized with Juwet leaf plant extract show a more precise shape than SEM results. The particles are spherical, with some areas showing aggregation. Higher magnification shows that the nanoparticles' size is 10–50 nm, with some larger particles due to agglomeration phenomena. Compared with conventional methods such as sol-gel or hydrothermal, synthesis using plant extracts can produce smaller particles but with a broader size distribution.

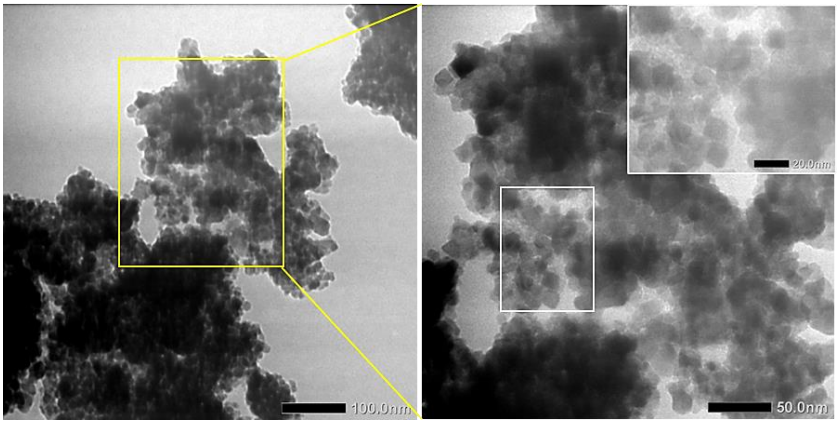

Figure 8 TEM characterization of TiO_2 nanoparticles (size ≈10-50 nm)

3.6 UV-Visible spectroscopic analysis

UV-visible characterization is used to determine the band gap energy value of TiO_2 nanoparticles. The results were obtained from UV-visible characterization using a wavelength spectrum with absorbance values. The UV-Vis spectrum in Figure 9 shows that the absorbance peak is at a wavelength of about 325-380 nm. From the wavelength and absorbance values that have been obtained, band gap energy will be sought. Band gap is the difference between the lower end of the valence band (+) and the upper end of the conduction band (-) or the minimum energy required to excite electrons from the valence band to the conduction band. The Tauc-plot method is a method for determining the band gap value by looking at a linear graph of the relationship E(eV) on the x-axis and $(\alpha h\upsilon)^{1/2}$ on the y-axis [25]. The results of TiO_2 band gap energy are shown in Figure 9 (insert). The Tauc-plot equation can be written as [55]:

$$D(hv - Eg) = (\alpha hv)^{\gamma} \quad (2)$$

Where, for a direct bandgap ($\gamma = 2$) and an indirect bandgap ($\gamma = 1/2$), α represents the absorption coefficient, $h\upsilon$ is the energy, Eg is the bandgap energy, and D is a constant.

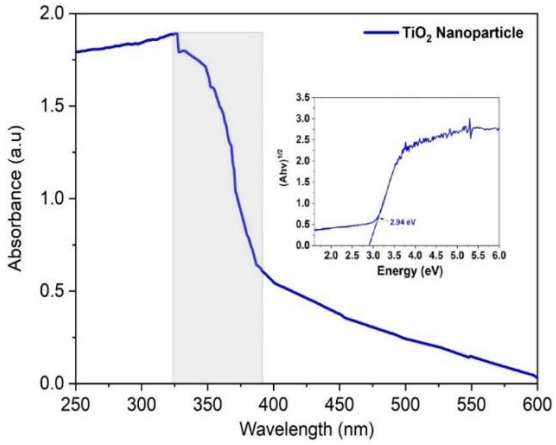

Figure 9 UV-Vis spectrum and indirect electronic transition (Eg) of TiO_2 NPs.

The bandgap energy is a crucial factor influencing the effectiveness of catalyst material formation. Based on Eq.2, the graph in Figure 9 (insert) shows that the bandgap energy of TiO_2 nanoparticles is 2.94 eV. This bandgap value is narrower than previously reported [33, 35, 52] because plant metabolites cap the TiO_2 NPs. During the green synthesis process (shown in Figure 2), this was confirmed by the analysis of functional groups such as C=C and C-OH (Figure 6). These results indicate that TiO_2 NPs, as semiconductor materials, can be efficient photocatalysts, reacting effectively when exposed to UV light. This is due to hydroxyl (OH) radicals forming, which play a key role in dye removal during the photocatalytic process [55].

3.7 Photocatalyst activity and UV-Vis test results of methylene blue

In photocatalytic activity, the band gap energy of semiconductor materials is important for the performance of electrons and holes to excite and recombine, which simultaneously intervene in reduction and oxidation (*redox*) activities. In addition to the band gap, it is also important to slow down the recombination process, which will impact optimal reduction and oxidation activities. The redox mechanism by holes in the valence band area (*ground state*) and electrons in the conduction band area (*excited state*) plays a role in the degradation process of the substrate in contact with the photocatalyst surface. Boles and electrons can produce reactive ions that are useful in deactivating and decomposing harmful contaminants or microorganisms. Electrons will react with air or oxygen (O_2) to form superoxide radicals (O_2^{-}*), while holes react with water molecules (H_2O) to form hydroxyl radicals (OH*) and H_2O^{+}. These radicals continue to form as long as the photocatalyst material is exposed to light or photons, and they decompose organic compounds into small molecules such as CO_2, H_2O, and mineral acids. This redox process (e^- and h^+) will continue and produce hydroxyl and superoxide radicals as long as the photocatalyst material is exposed to light to degrade the dye molecules and decompose into vaporized gas [55].

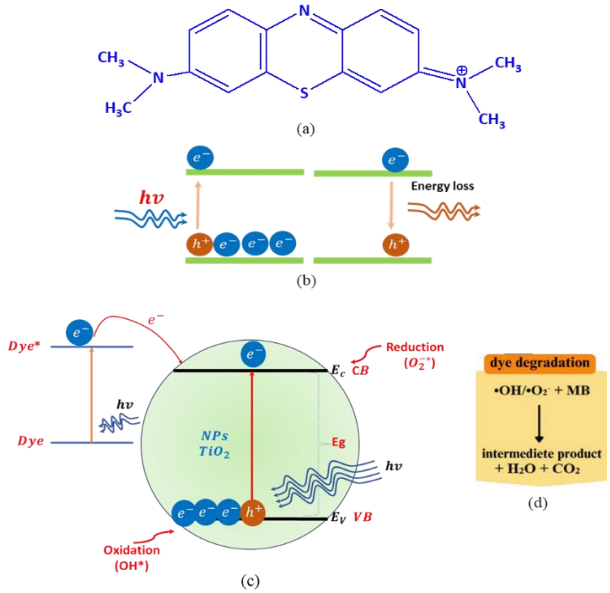

Figure 10 Illustration of the molecular structure of dyes (a), interaction of semiconductors with photons: excitation and recombination with absorption and release of energy (hv)(a), photocatalysis process on TiO_2 NPs for dye degradation (b), stages of MB degradation by TiO_2 NPs(c).

As shown in Figure 10, semiconductor materials with a smaller bandgap require less photon energy to excite electrons from the valence band to the conduction band, resulting in a faster absorption process. Pure anatase TiO_2 is limited to photocatalytic activity only in the UV region of solar energy (i.e., Eg = 2.94 eV and λ: 325-380 nm), which utilizes only 5% of the solar spectrum. Compared to rutile and brookite phases, anatase is the most effective TiO_2 phase for photocatalysis. Its wider bandgap leads to a lower electron-

hole recombination rate, making it more efficient in generating reactive radicals for contaminant degradation. Reactive oxygen species (ROS) produced during the photocatalytic process are primarily superoxide radicals ($O_2^{\bullet-}$) and hydroxyl radicals (•OH). However, other species, such as hydroperoxide radicals (•OOH) and hydrogen peroxide (H_2O_2), can also form through further oxidation, dimerization, or disproportionation processes [55].

Figure 10 illustrates the TiO_2 photocatalytic reaction, where CB and CV represent the conduction and valence bands, respectively. Eq.3 shows the gap energy of the TiO_2 semiconductor, and Eq.4 shows the formation of free electrons and holes, where e^-, hv, and represent the electrons in the conduction band, photon energy, and holes in the valence band, respectively. When a TiO_2 semiconductor receives energy greater than its band gap energy (E_g), electrons will move from the valence band to the conduction band, thus forming holes (h^+) in the valence band and electrons (e^-) in the conduction band [56]. These excited electrons can reduce various substrates or react with oxygen (O_2) on the semiconductor surface or in water, then reduce it to superoxide radical anions ($O_2^{-}\bullet$) (Eq.6). Meanwhile, holes can oxidize organic molecules to form R^+, or react with hydroxide ions (OH^-) or water (H_2O), producing hydroxyl radicals (HO•) (Eq.5). Peroxide radicals as strong oxidants also play a role in the photodecomposition process of organic substrates. Hydroxyl radicals (HO•) and superoxide ($O_2^{-}\bullet$) are powerful oxidizers and reductants, capable of oxidizing and reducing most pollutants to carbon dioxide and water (Eq.7-8). Furthermore, electron-hole recombination releases energy to produce heat (Eq.9); as long as electrons receive the photon energy in the valence band, the photocatalytic process will occur continuously [31, 55, 57].

$$E_g = E_C - E_V \tag{3}$$

$$Photocatalysis\ (TiO_2) + hv \rightarrow e_{\mathrm{cb}}^- + h_{\mathrm{vb}}^+ \tag{4}$$

$$h_{vb}^+ + H_2O \rightarrow H^+ + HO^*(hydroxile\ radical) \tag{5}$$

$$e_{cb}^- + O_2 \rightarrow O_2^{-*}(superoxide\ radical) \tag{6}$$

$$HO^* + Pollutant\ (MB) \rightarrow H_2O + CO_2 \tag{7}$$

$$O_2^* + Pollutant\ (MB) \rightarrow H_2O + CO_2 \tag{8}$$

$$e_{cb}^- + h_{\mathrm{vb}}^+ \rightarrow heat \tag{9}$$

Equations 4-8 illustrate the reactions involved in the photocatalytic process, including photoexcitation, electron injection, and dye regeneration. Equations 10-12 describe the stages of the process. Hydroxyl radicals and superoxide ions formed during photocatalysis attack organic pollutant molecules (such as dyes or hazardous chemical compounds), breaking them down into simpler compounds, such as carbon dioxide (CO_2) and water (H_2O) [57-59].

$$O_2^{-*} + H^+ \rightarrow HO_2^* \tag{10}$$

$$HO_2^* + HO_2^* \rightarrow H_2O_2 + O_2 \tag{11}$$

$$R + HO^* \rightarrow CO_2 + H_2O \tag{12}$$

In the process of photocatalyst activity, a methylene blue concentration of 30 ppm with a catalyst mass of 10 mg in 50 ml of TiO_2 was used. The research was conducted by giving time variations of 60 minutes, 120 minutes, 180 minutes, and 240 minutes. The testing process was done by mixing the catalyst into the methylene blue solution, stirring it into the dark for 1 hour, and continuing the irradiation process. The irradiation used in this study is with ultraviolet light, and the results of the methylene blue solution with variations in irradiation time can be seen in Figure 11. Based on this Figure, it can be seen that the longer the irradiation time, the more the methylene blue solution fades.

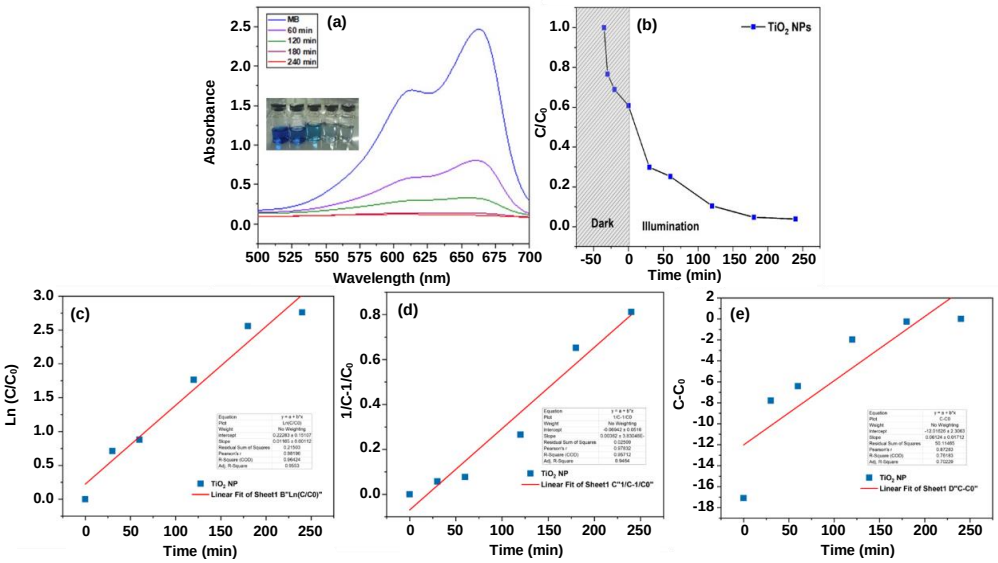

Figure 11 UV-Visible spectrum of MB with TiO_2 catalyst (a); degradation of MB by TiO_2 NPs (b). Kinetic Plot of TiO_2 NPs: First Order (c), Second Order (d), and Zero Order (e)

Table 3 Some Values of Photocatalytic Kinetic Models of MB with Various Photocatalysts

Absorbent	Adsorbate	Order 0		Order 1		Order 2	
		R_2	K_0 (min^{-1})	R_2	K_1 (min^{-1})	R_2	K_2 (min^{-1})
TiO_2 NP	**MB**	0.7618	0.06124	0.96424	0.01125	0.95712	0.00362

After the photocatalytic activity process, the percentage of methylene blue (MB) degradation will be determined using UV-visible spectroscopy. The data obtained from the UV-visible test consists of the spectrum showing the relationship between wavelength and absorbance, as shown in Figure 11(a) for MB with the TiO_2 catalyst, and Figure 11(b), which presents the C/C_0 versus time curve. The spectrum reveals that as the irradiation time increases, the absorbance value of methylene blue decreases, indicating that ultraviolet light reduces the absorbance. Based on the analysis, the degradation of MB with TiO_2 nanoparticles follows a pseudo-first-order kinetic model, which is common in photocatalytic reactions. The $Ln(C/C_0)$ vs. time graph (Figure 11c) shows a linear relationship, indicating that the pollutant concentration is much smaller than the number of active sites on the photocatalyst surface, so the number of available active sites remains almost constant. Under this condition, the reaction rate depends only on the pollutant concentration, so first-order kinetics can be applied. Choosing an appropriate kinetic model is important to determine the photocatalyst's reaction mechanism and effectiveness (Table 3) [60].

The concentration after using a standard curve of methylene blue was determined, and the standard curve used in this study was two ppm to 20 ppm. Through the calculation of equations 2 and 3, the methylene blue concentration value after irradiation and the percentage degradation. Based on these data, it is known that the longer the irradiation contact time, the lower the concentration of methylene blue solution, so the longer the irradiation time, the greater the percentage of degradation of methylene blue [61]. With the time variation, the optimal time for methylene blue to degrade using UV light can be determined. The TiO_2 nanoparticles can determine the effectiveness of the material in the photocatalyst process of methylene blue degradation. Figure 12 shows the graph between time and percentage degradation; it can be seen that on the TiO_2 catalyst at 60 minutes, the degraded methylene blue solution reached 74%, and at 240 minutes, it reached 95.40% [42]. Compared with other previously reported photocatalysts (Table 4), Figure 12 shows that methylene blue (MB) was degraded by 40% at 0 minutes, likely due to the physicochemical interactions between TiO_2 and MB before full photocatalysis. Adsorption is crucial, as pollutant molecules (like MB) must adhere to the photocatalyst surface to interact with reactive species such as hydroxyl radicals (*OH) generated during photocatalysis. Significant adsorption on the TiO_2 surface can trigger direct redox reactions with active sites or functional groups on TiO_2, even before light energy is absorbed to generate electron-hole pairs [57, 62, 63].

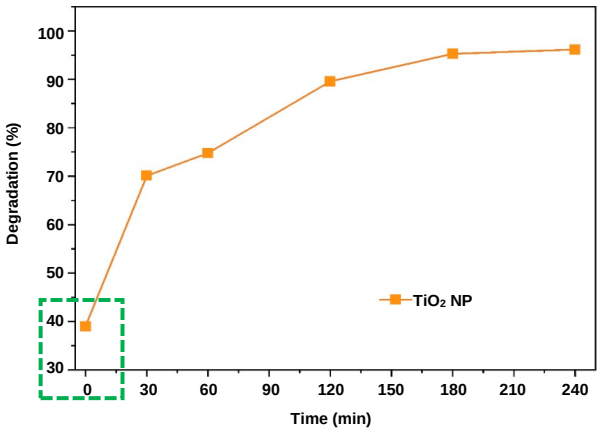

Figure 12 Effect of UV irradiation time on MB degradation percentage

Table 4 Comparison of the Photocatalytic Performance of TiO_2 Nanocomposites with Other Photocatalyst

Photo-catalyst	Pollutant	Synthesis Method	Efficiency degradation (%)	Time (min)	Condition	Ref
TiO_2	MB	Sol-gel	62	150	100 mg, 100 mg/L MB, UV lamp	[64]
TiO_2	MB	Microwave assisted	81.65	60	100 mL MB, 10 mg/L, 50 mg, UV lamp	[65]
TiO_2	MB	Hydrothermal	65	90	200 mL MB, 36 W UV-C lamp	[66]
TiO_2	MB	*Acalypha indica*	86	35	100 mL MB, 10mg/L, 25 W Phillips lamp	[67]
TiO_2	MB	*Aloe vera*	94	120	100 mL MB, 10 mg, UV lamps	[68]
TiO_2	lead (Pb)	*Syzygium cumini*	82.53	720	500 mL, UV lamps of 15 W	[36]
TiO_2	MB	*Syzygium cumini*	**97.2**	240	25 mL MB, 30 mg/L, 12 W UV-LED	**This work**

TiO_2 nanoparticles (NPs) act as photocatalysts to degrade dyes through a process that involves several key steps triggered by UV light irradiation. When TiO_2 is exposed to UV light with energy greater than its bandgap (≈2.94 eV), electrons in the valence band are excited to the conduction band, leaving behind holes in the valence band. The excited electrons (e^-) and holes (h^+) can interact with surrounding molecules. Electrons in the conduction band react with oxygen (O_2) on the surface to form superoxide radicals ($\bullet O_2^-$). In contrast, holes in the valence band can oxidize water (H_2O) or hydroxide ions (OH^-) to generate hydroxyl radicals (•OH), which are strong oxidants. Dyes, such as methylene blue (MB), adsorbed on the TiO_2 surface, are then oxidized by hydroxyl radicals (•OH) and may also be oxidized directly by holes (h^+) on TiO_2. These reactions break down the dye molecules into smaller compounds, such as CO_2, H_2O, and other simpler ions. The efficiency of the degradation process depends on various factors, including the size of the TiO_2

particles, surface area, UV light intensity, and oxygen concentration. Furthermore, the presence of superoxide radicals ($\bullet O_2^-$) and hydroxyl radicals (•OH) plays a crucial role in accelerating the cleavage of chemical bonds in the dye molecules [33, 55].

4. Conclusion

This study successfully synthesized TiO_2 NPs using juwet leaf extract as a natural reducing agent. Characterization showed that the resulting nanoparticles had an anatase phase with high purity (98.21%), nearly spherical morphology with an average size of range of 10–50 nm, and a bandgap energy of 2.94 eV, which was narrower than conventional TiO_2. Photocatalytic tests using methylene blue solution showed high degradation efficiency, reaching 94.92% in 180 minutes and increasing to 95.89% after 240 minutes of UV exposure. Compared with conventional synthesis methods such as sol-gel or hydrothermal, this green synthesis method offers a more environmentally friendly approach while maintaining high pollutant degradation effectiveness. With these results, the synthesis of TiO_2 NPs based on plant extracts shows excellent potential for photocatalytic applications in water purification and industrial wastewater treatment. Further optimization of synthesis parameters and structural modifications can improve the stability and pollutant degradation efficiency for wider applications. Further studies on electron transfer and pollutant interactions will provide better insight into their photocatalytic performance.

5. Acknowledgments

The author wishes to thank the State University of Surabaya (UNESA) for financially supporting this research (Contract Number: 32147/UN38.3/LK04.00/2024). Special thanks are also extended to the Material Physics Laboratory, Department of Physics, Faculty of Mathematics and Natural Sciences, UNESA, for their invaluable assistance in synthesizing TiO_2 nanoparticles.

6. References

[1] Kedzior SB. Clean water and universal sanitation in an Era of sustainable development: understanding the challenges and prospects for SDG 6 in the Ganga River Basin. In: Dutta V, Ghosh P, editors. Sustainability: Science, Policy, and Practice in India. Sustainable Development Goals Series. Cham: Springer; 2023. p. 85-103.

[2] Milan BF. Clean water and sanitation for all: interactions with other sustainable development goals. Sustain Water Resour Manag. 2017;3(4):479-89.

[3] Chowdhary P, Bharagava RN, Mishra S, Khan N. Role of industries in water scarcity and its adverse effects on environment and human health. In: Shukla V, Kumar N, editors. Environmental Concerns and Sustainable Development. Singapore: Springer; 2020. p. 235-56.

[4] Adyasari D, Pratama MA, Teguh NA, Sabdaningsih A, Kusumaningtyas MA, Dimova N. Anthropogenic impact on Indonesian coastal water and ecosystems: current status and future opportunities. Mar Pollut Bull. 2021;171:112689.

[5] Murgolo S, De Ceglie C, Di Iaconi C, Mascolo G. Novel TiO_2-based catalysts employed in photocatalysis and photoelectrocatalysis for effective degradation of pharmaceuticals (PhACs) in water: a short review. Curr Opin Green Sustain Chem. 2021;30:100473.

[6] Ahmadpour N, Nowrouzi M, Avargani VM, Sayadi MH, Zendehboudi S. Design and optimization of TiO_2-based photocatalysts for efficient removal of pharmaceutical pollutants in water: recent developments and challenges. J Water Process Eng. 2024;57:104597.

[7] Maqbool Q, Czerwinska N, Giosue C, Sabbatini S, Ruello ML, Tittarelli F. New waste-derived TiO_2 nanoparticles as a potential photocatalytic additive for lime based indoor finishings. J Clean Prod. 2022;373:133853.

[8] Kalse SB, Swami SB. Recent application of jackfruit waste in food and material engineering: a review. Food Biosci. 2022;48:101740.

[9] Narath S, Koroth SK, Shankar SS, George B, Mutta V, Wacławek S, et al. *Cinnamomum tamala* leaf extract stabilized zinc oxide nanoparticles: a promising photocatalyst for methylene blue degradation. Nanomaterials. 2021;11(6):1558.

[10] Khoirotin, Faaizatunnisa N, Munasir. Green synthesis of Fe_3O_4 nanoparticles using green betel leaf extract for methylene blue adsorption. Nat Life Sci Commun. 2023;22(3):e2023042.

[11] Bassim S, Mageed AK, AbdulRazak AA, Al-Sheikh F. Photodegradation of methylene blue with aid of green synthesis of CuO/TiO_2 nanoparticles from extract of citrus aurantium juice. Bull Chem React Eng Catal. 2023;18(1):1-16.

[12] Sarkar Phyllis AK, Tortora G, Johnson I. Photodegradation. In: Sarkar Phyllis AK, Tortora G, Johnson I, editors. The Fairchild Books Dictionary of Textiles. New York: Bloomsbury Publishing; 2022.

[13] Hanafi MF, Sapawe N. A review on the water problem associate with organic pollutants derived from phenol, methyl orange, and remazol brilliant blue dyes. Mater Today: Proc. 2020;31:A141-50.

[14] Faaizatunnisa N, Ediati R, Fansuri H, Juwono H, Suprapto S, Hidayat ARP, et al. Facile green synthesis of core–shell magnetic MOF composites (Fe_3O_4@SiO_2@HKUST-1) for enhanced adsorption capacity of methylene blue. Nano-Struct Nano-Objects. 2023;34:100968.

[15] Bassim S, Mageed AK, AbdulRazak AA, Majdi HS. Green synthesis of Fe_3O_4 Nanoparticles and its applications in wastewater treatment. Inorganics. 2022;10(12):260.

[16] Verma V, Al-Dossari M, Singh J, Rawat M, Kordy MGM, Shaban M. A review on green synthesis of TiO_2 NPs: synthesis and applications in photocatalysis and antimicrobial. Polymers (Basel). 2022;14(7):1444.

[17] Faaizatunnisa N, Ediati R, Yusof ENM, Fadlan A, Karelius K, Kulsum U, et al. The mixed-ligand strategy for structural modification of MOF materials to enhance the photocatalytic degradation and adsorption of organic pollutants: a review. Nano-Struct Nano-Objects. 2024;40:101366.

[18] Dastan D, Chaure NB. Influence of surfactants on TiO_2 nanoparticles grown by sol-gel technique. Int J Mater Mech Manuf. 2014;2(1):21-4.

[19] Okto SHS, As'adah A, Putri AR, Basmalah M, Munasir M. Green synthesis of TiO_2 nanoparticles from Juwet leaf extract (*Syzygium cumini*) as a photocatalytic material: removing ion-Pb in industrial wastewater. Prosiding Seminar Nasional Unimus. 2022;5:647-56. (In Indonesian)

[20] Ali K, Dwivedi S, Azam A, Saquib Q, Al-Said MS, Alkhedhairy AA, et al. Aloe vera extract functionalized zinc oxide nanoparticles as nanoantibiotics against multi-drug resistant clinical bacterial isolates. J Colloid Interface Sci. 2016;472:145-56.
[21] Vinayagam R, Batra S, Murugesan G, Goveas LC, Varadavenkatesan T, Menezes A, et al. Emerging contaminant removal using eco-friendly zinc ferrite nanoparticles: sunlight-driven degradation of tetracycline. Emerg Contam. 2025;11(2):100469.
[22] Li Y, Fu Y, Zhu M. Green synthesis of 3D tripyramid TiO_2 architectures with assistance of aloe extracts for highly efficient photocatalytic degradation of antibiotic ciprofloxacin. Appl Catal B Environ. 2020;260:118149.
[23] Anbumani D, Dhandapani KV, Manoharan J, Babujanarthanam R, Bashir AKH, Muthusamy K, et al. Green synthesis and antimicrobial efficacy of titanium dioxide nanoparticles using *Luffa acutangula* leaf extract. J King Saud Univ Sci. 2022;34(3):101896.
[24] Huamán A, Salazar K, Quintana M. Molecular interaction of natural dye based on *Zea mays* and *Bixa orellana* with nanocrystalline TiO_2 in dye sensitized solar cells. J Electrochem Sci Eng. 2021;11(3):179-95.
[25] Nabi G, Majid A, Riaz A, Alharbi T, Kamran MA, Al-Habardi M. Green synthesis of spherical TiO_2 nanoparticles using *Citrus Limetta* extract: excellent photocatalytic water decontamination agent for RhB dye. Inorg Chem Commun. 2021;129:108618.
[26] Pushpamalini T, Keerthana M, Sangavi R, Nagaraj A, Kamaraj P. Comparative analysis of green synthesis of TiO_2 nanoparticles using four different leaf extract. Mater Today: Proc. 2021;40:S180-4.
[27] Krisdiyanto D, Khuzaifah S, Khamidinal K, Sedyadi E, et al. Influence of dye adsorbtion time on TiO_2 dye-sensitized solar cell with krokot extract (*Portulaca Oleracea*. L) as a natural sensitizer. J Pure Appl Chem Res. 2015;4(1):17-24.
[28] Vembu S, Vijayakumar S, Nilavukkarasi M, Vidhya E, Punitha VN. Phytosynthesis of TiO_2 nanoparticles in diverse applications: what is the exact mechanism of action?. Sens Int. 2022;3:100161.
[29] Selvaraj R, Nagendran V, Varadavenkatesan T, Goveas LC, Vinayagam R. Stable silver nanoparticles synthesis using *Tabebuia aurea* leaf extract for efficient water treatment: a sustainable approach to environmental remediation. Chem Eng Res Des. 2024;208:456-63.
[30] Ghosh S, Das AP. Modified titanium oxide (TiO_2) nanocomposites and its array of applications: a review. Toxicol Environ Chem. 2015;97(5):491-514.
[31] Maurya IC, Singh S, Senapati S, Srivastava P, Bahadur L. Green synthesis of TiO_2 nanoparticles using *Bixa orellana* seed extract and its application for solar cells. Sol Energy. 2019;194:952-8.
[32] Varadavenkatesan T, Nagendran V, Vinayagam R, Goveas LC, Selvaraj R. Effective degradation of dyes using silver nanoparticles synthesized from *Thunbergia grandiflora* leaf extract. Bioresour Technol Rep. 2024;27:101914.
[33] Eddy DR, Permana MD, Sakti LK, Sheha GAN, Solihudin, Hidayat S, et al. Heterophase Polymorph of TiO_2 (Anatase, Rutile, Brookite, TiO_2 (B)) for efficient photocatalyst: fabrication and activity. Nanomaterials. 2023;13(4):704.
[34] Koelsch M, Cassaignon S, Guillemoles JF, Jolivet JP. Comparison of optical and electrochemical properties of anatase and brookite TiO_2 synthesized by the sol-gel method. Thin Solid Films. 2002;403-404:312-9.
[35] Allen NS, Mahdjoub N, Vishnyakov V, Kelly PJ, Kriek RJ. The effect of crystalline phase (anatase, brookite and rutile) and size on the photocatalytic activity of calcined polymorphic titanium dioxide (TiO_2). Polym Degrad Stab. 2018;150:31-6.
[36] Sethy NK, Arif Z, Mishra PK, Kumar P. Green synthesis of TiO_2 nanoparticles from *Syzygium cumini* extract for photocatalytic removal of lead (Pb) in explosive industrial wastewater. Green Process Synth. 2020;9(1):171-81.
[37] Kharat SN, Mendhulkar VD. Synthesis, characterization and studies on antioxidant activity of silver nanoparticles using *Elephantopus scaber* leaf extract. Mater Sci Eng C Mater Biol Appl. 2016;62:719-24.
[38] Sunny NE, Mathew SS, Chandel N, Saravanan P, Rajeshkannan R, Rajasimman M, et al. Green synthesis of titanium dioxide nanoparticles using plant biomass and their applications- a review. Chemosphere. 2022;300:134612.
[39] Tien TWH, Rasmiyanti NKE, Tandi J, Magfirah. Total secondary metabolites and test of antioxidant activity of juwet leaves (*Syzygium cumini* L.) with Uv-Vis spectrophotometer. KOVALEN: Jurnal Riset Kimia. 2023;9(3):295-304. (In Indonesia)
[40] Jagetia GC. Bioactive phytoconstituents and medicinal properties of Jamun (*Syzygium cumini*). J Explor Res Pharmacol. 2024;9(3):180-212.
[41] Zhang H, Banfield JF. Understanding polymorphic phase transformation behavior during growth of nanocrystalline aggregates: insights from TiO_2. J Phys Chem B. 2000;104(15):3481-7.
[42] Sharma M, Behl K, Nigam S, Joshi M. TiO_2-GO nanocomposite for photocatalysis and environmental applications: a green synthesis approach. Vacuum. 2018;156:434-9.
[43] Munasir N, Kusumawati RP, Kusumawati DH, Supardi ZAI, Taufiq A, Darminto. Characterization of Fe_3O_4/rGO composites from natural sources: application for dyes color degradation in aqueous solution. Int J Eng Trans A: Basics. 2020;33(1):18-27.
[44] Bai J, Zhou B. Titanium dioxide nanomaterials for sensor applications. Chem Rev. 2014;114(19):10131-76.
[45] Eshwarappa RSB, Iyer RS, Subbaramaiah SR, Richard SA, Dhananjaya BL. Antioxidant activity of *Syzygium cumini* leaf gall extracts. Bioimpacts. 2014;4(2):101-7.
[46] Banerjee A, Dasgupta N, De B. In vitro study of antioxidant activity of *Syzygium cumini* fruit. Food Chem. 2005;90(4):727-33.
[47] da Rosa ACS, Hoscheid J, Garcia VAdS, de Oliveira Santos Junior O, da Silva C. Phytochemical extract from *Syzygium cumini* leaf: maximization of compound extraction, chemical characterization, antidiabetic and antibacterial activity, and cell viability. Processes 2024;12(10):2270.
[48] Djerdj I, Tonejc AM. Structural investigations of nanocrystalline TiO_2 samples. J Alloys Compd. 2006;413(1-2):159-74.
[49] You YF, Xu CH, Xu SS, Cao S, Wang JP, Huang YB, et al. Structural characterization and optical property of TiO_2 powders prepared by the sol–gel method. Ceram Int. 2014;40(6):8659-66.
[50] Jalaukhan AHA. Optical investigation of TiO_2/graphene oxide thinfilm prepared by spin coating technique. IOP Conf Ser: Mater Sci Eng. 2020;871:012087.
[51] Dodoo-Arhin D, Buabeng FP, Mwabora JM, Amaniampong PN, Agbe H, Nyankson E, et al. The effect of titanium dioxide synthesis technique and its photocatalytic degradation of organic dye pollutants. Heliyon. 2018; 4(7):e00681.
[52] Habibi Jetani G, Rahmani MB. TiO_2/GO nanocomposites: synthesis, characterization, and DSSC application. Eur Phys J Plus. 2020;135(9):720.
[53] Ola O, Maroto-Valer MM. Review of material design and reactor engineering on TiO_2 photocatalysis for CO_2 reduction. J Photochem Photobiol C: Photochem Rev. 2015;24:16-42.

[54] Perumalsamy H, Balusamy SR, Sukweenadhi J, Nag S, MubarakAli D, El-Agamy Farh M, et al. A comprehensive review on *Moringa oleifera* nanoparticles: importance of polyphenols in nanoparticle synthesis, nanoparticle efficacy and their applications. J Nanobiotechnol. 2024;22:71.
[55] Žerjav G, Žižek K, Zavašnik J, Pintar A. Brookite vs. rutile vs. anatase: what`s behind their various photocatalytic activities?. J Environ Chem Eng. 2022;10(3):107722.
[56] Nasikhudin, Diantoro M, Kusumaatmaja A, Triyana K. Study on photocatalytic properties of TiO_2 nanoparticle in various pH condition. J Phys Conf: Ser. 2018;1011:012069.
[57] Schneider J, Matsuoka M, Takeuchi M, Zhang J, Horiuchi Y, Anpo M, et al. Understanding TiO_2 photocatalysis: mechanisms and materials. Chem Rev. 2014;114(19):9919-86.
[58] Islam Molla MA, Tateishi I, Furukawa M, Katsumata H, Suzuki T, Kaneco S. Evaluation of reaction mechanism for photocatalytic degradation of dye with self-sensitized TiO under visible light irradiation. Open J Inorg Non-Met Mater. 2017;7(1):1-7.
[59] Nosaka Y, Nosaka A. Understanding hydroxyl radical (•OH) generation processes in photocatalysis. ACS Energy Lett. 2016;1(2):356-9.
[60] Wang R, Shi K, Huang D, Zhang J, An S. Synthesis and degradation kinetics of TiO_2/GO composites with highly efficient activity for adsorption and photocatalytic degradation of MB. Sci Rep. 2019;9:18744.
[61] Saranya KS, Padil VVT, Senan C, Pilankatta R, Saranya SK, George B, et al. Green synthesis of high temperature stable anatase titanium dioxide nanoparticles using gum kondagogu: characterization and solar driven photocatalytic degradation of organic dye. Nanomaterials. 2018;8(12):1002.
[62] Mittal P, Bansal R. Role of cross-disciplinary collaborations for holistic approach to sustainability bt- community engagement for sustainable practices in higher education: from awareness to action. In: Mittal P, Bansal R, editors. Community Engagement for Sustainable Practices in Higher Education. Cham: Palgrave Macmillan; 2024; p. 143-60.
[63] Cai Y, Feng YP. Review on charge transfer and chemical activity of TiO_2: Mechanism and applications. Prog Surf Sci. 2016;91(4):183-202.
[64] Gautam A, Kshirsagar A, Biswas R, Banerjee S, Khanna PK. Photodegradation of organic dyes based on anatase and rutile TiO_2 nanoparticles. RSC Adv. 2016;6(4):2746-59.
[65] Almashhori K, Ali TT, Saeed A, Alwafi R, Aly M, Al-Hazmi FE. Antibacterial and photocatalytic activities of controllable (anatase/rutile) mixed phase TiO_2 nanophotocatalysts synthesized: via a microwave-assisted sol-gel method. New J Chem. 2020;44(2):562-70.
[66] Mustapha FH, Jalil AA, Mohamed M, Triwahyono S, Hassan NS, Khusnun NF, et al. New insight into self-modified surfaces with defect-rich rutile TiO_2 as a visible-light-driven photocatalyst. J Clean Prod. 2017;168:1150-62.
[67] Latif S, Tahir K, Khan AU, Abdulaziz F, Arooj A, Alanazi TYA, et al. Green synthesis of Mn-doped TiO_2 nanoparticles and investigating the influence of dopant concentration on the photocatalytic activity. Inorg Chem Commun. 2022;146:110091.
[68] Srujana S, Anjamma M, Alimuddin, Singh B, Dhakar RC, Natarajan S, et al. A comprehensive study on the synthesis and characterization of TiO_2 nanoparticles using aloe vera plant extract and their photocatalytic activity against MB dye. Adsorpt Sci Technol. 2022;2022:7244006.